Response Builders of MAXI X-ray Slit Cameras and Simulator

Mutsumi Sugizaki on behalf of MAXI Software Team

RIKEN, 2-1 Hirosawa, Wako, Saitama, 351-0198, Japan
E-mail(MS): sugizaki@riken.jp

Abstract

MAXI, an all-sky X-ray monitor to be on-board on the ISS (International Space Station), carries two kinds of X-ray cameras: GSC (Gas Slit Camera) and SSC (Solid-state Slit Camera). Both X-ray cameras are scanning imagers combining position-sensitive detectors and collimators with one-dimensional FOV (field of view). They covers 90% of the whole sky every 90 minutes of the ISS orbital period. The response functions of these cameras for any X-ray sources on the sky depends on the ISS attitude, which always varies according to the orbital motion of the ISS. We are developing software to build response functions for any X-ray source on the sky from the source position coordinates, the instrument calibration data, and the ISS configuration parameters. We introduce the standard scheme of the MAXI data analysis and the response builders used in it. We then present the preliminary results of the response builders and the observation simulator which are currently being developed.

Key words: Methods: data analysis — ISS: All Sky Monitor — MAXI

1. Introduction

MAXI is a mission carried on the ISS to monitor all-sky X-ray image (ref. Ueno et al. 2004; Matsuoka et al. 2007; Ueno et al. in this proceedings). It onboards two kinds of X-ray cameras: GSC (Mihara et al. 2001; Mihara et al. in this proceedings) and SSC (Katayama et al. 2005; Tomida et al. in this proceedings). Both X-ray cameras are slit cameras with one-dimensional FOVs and scan the whole sky according to the rotation of the ISS synchronized with the orbital motion.

The response functions of the GSC and the SSC for any X-ray source depend on the ISS attitude, which is always changing according to the ISS orbital motion. The ISS activities, such as motions of the astronauts, rotations of the Solar-buttery paddles, docking with transfer vehicles, can also affect the ISS motion and sometimes interfere the FOVs of the X-ray cameras. These situations are quite different from those in the pointing X-ray telescopes onboard solitary astronomical satellite. The environmental issues specific to the ISS have to be cared in the MAXI data analysis.

We are developing software for the MAXI data analysis, which includes programs for telemetry-data reduction, response builders, and an observation simulator. In this paper, we briefly introduce the principle of the MAXI all-sky observation and describe the scheme of the standard data-analysis. We then present the preliminary results obtained using the response builders and the observation simulator which are now under development.

2. Principle of MAXI All-Sky Observation

Figure 1 illustrates the principle of the MAXI all-sky observation. Both X-ray cameras, GSC and SSC, are one-dimensional slit cameras. Each camera unit consists of a slat collimator with a narrow open window at the top and a position sensitive detector at the bottom. GSC employs position-sensitive gas proportional counters as the detector, whereas SSC employs CCD arrays. The one-dimensional FOVs of each camera scans the sky according to the rotation of the ISS. The cycle is synchronized with the orbital motion of about 90-minute period around the earth. Both GSC and SSC are segmented into the horizon units and the zenith units. The FOVs of the horizon units are towards the ISS moving direction along the earth horizon, and those of the zenith units are towards the anti-earth direction. Figure 2 shows the collimator effective-area profiles of one-dimensional FOVs of each GSC/SSC units. The combination of the two-segmental units scans the 90% of the whole sky twice per one orbital period of about 90 minutes.

3. Data Analysis Scheme

Figure 3 illustrate the schematic of the the MAXI data analysis from the telemetry data. The analysis flow is largely divided into two sections: the telemetry data reduction and the science analysis, whose processes are described in the following subsections. We employ relational-database system to store all the telemetry data in order to maximize the efficiency of the data reduction and analysis.

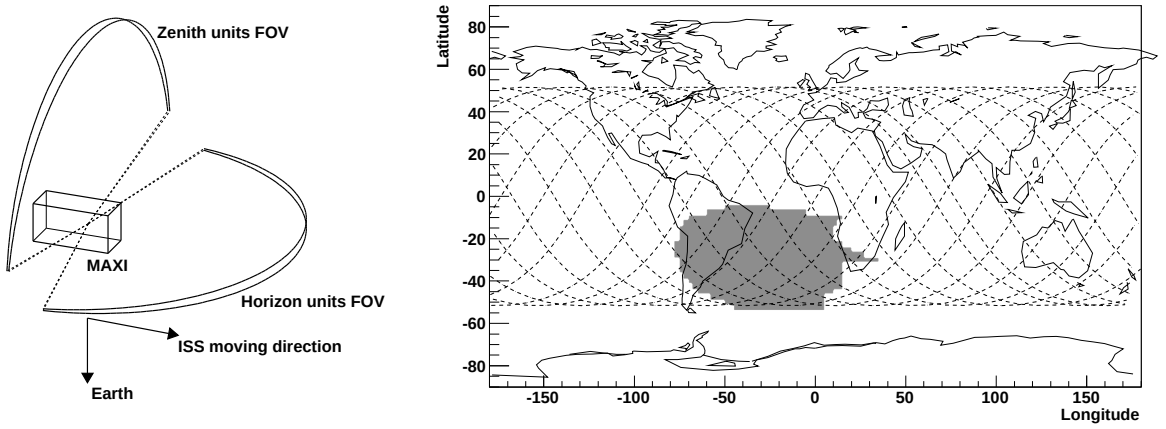

Fig. 1. Field of views of X-ray slit cameras on MAXI and direction of the ISS orbital motion (left). Trajectory of ISS orbital motion for one day (right). Grey area on the south Atlantic ocean represents the GSC SAA where the GSC counters are turned off.

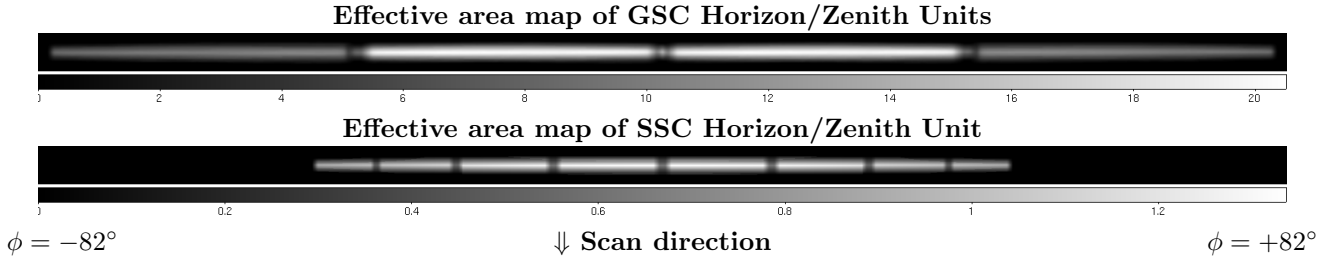

Fig. 2. Collimator effective-area map of GSC and SSC Horizon/Zenith units for incident angle. Units of grey scales are [cm^2]. Both images show the area of $-82° < \phi < 82°$ (along the direction parallel to the one-dimensional FOV) and $-2.5° < \theta < 2.5°$ (along the scan direction). The dips of the profiles corresponds to the detector insensitive areas, which are the shadows of the support structure of gas cells in GSC and the gaps between the CCD arrays in SSC.

3.1. Data Reduction

All the telemetry data are stored into database after the first reduction process. The database includes X-ray event data as well as auxiliary monitor data consisting of various housekeeping data and environmental information.

The event database stores all parameters relevant to each event such as the arrival time, the detector position, the incident angle, the expected sky position, and deposit energy. Some of these parameters are calculated during the reduction process using the instrument calibration data and the auxiliary monitor data.

The auxiliary monitor database collects information regarding the status of the ISS and the MAXI operation such as the ISS orbit and attitude parameters, configuration of the Solar-buttery paddles, temperatures of X-ray detectors and electronics, the mode of the data processor, data of radiation monitors, and so on.

The data-reduction process also requires the instrument calibration data. The calibration database are created from the ground calibration-test data and the in-orbit observation data. We employ the HEASARC CALDB system to be able to use the versatile management tool and provide the standard interface to software developers.

MAXI onboards two equipments to monitor the own attitude, VSC (Visual Star Camera) and RLG (Ring Laser Gyroscope), which work complimentarily. The attitude parameters are coarsely determined in orbit for the on-board realtime process, which are used in the quick nova-alert system. The parameters are then updated on the ground using the both VSC and RLG data after the downlink of all the relevant telemetry data is completed.

3.2. Science Analysis

The science analysis of MAXI data starts with the event selection for the target from the all-sky data. The event file for a target X-ray source is extracted from the event database, where the auxiliary monitor data is used to filter the events with various selection criteria. These database employ the relational database system in order to select the target events from the all-sky data efficiently and apply the flexible event-selection criteria.

Light curves, images, and energy spectra for the target X-ray source are then extracted from the event file. These products will be opened to public when the MAXI

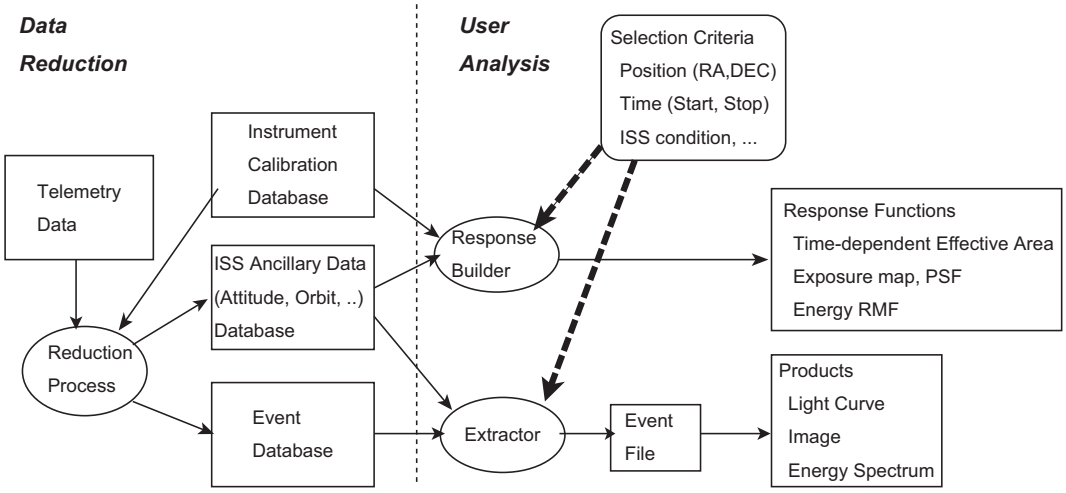

Fig. 3. Schematic of MAXI data analysis flow

mission is shifted into the normal operation phase (Kohama et al. in this proceedings).

The response builders calculate the response files for these light curves, energy spectra, and images from the instrument calibration data and the auxiliary monitor data. These details are described in the next section.

4. Response Builders

We here introduce the response builder of light curves, energy spectra, and images to be used in the standard analysis and show the preliminary results obtained using the programs under development. We used the instrument calibration data obtained from the ground experiments and assume the environmental parameters of ISS and MAXI expected from the current ISS configuration and orbits in 2007.

4.1. Light curve

The visibility and effective area of MAXI X-ray cameras for a given X-ray source are calculated from the source coordinates, the ISS position and configuration, transmission function of the slit collimators and the detector efficiency. The light-curve response builder calculates the effective area as a function of the time from these data.

Figure 4 shows the time variation of the GSC slit-collimator area for a point source at a given position (Crab nebula), obtained using the response builder. In the short time scale, the triangular response of the slat collimator with a duration of $\sim$45 seconds is clearly seen. The variation of the average exposure time per orbit (top panel of Figure 4) are caused by the variation of the source incident angle within the FOV due to the precession of the ISS orbit. The dips on the profile correspond to the down time for SAA and Sun area as well as the shadows of the support structures in detector areas.

4.2. Energy spectrum

The energy response function is represented by the effective area and the dispersion relation between the energy and the pulse height of the detector signal. The energy dispersion is owing to the X-ray detectors. GSC utilizes the gas proportional counters, whereas SSC utilizes CCD.

The effective area of the collimators and the detectors depends on the X-ray incident angle. Figure 5 shows the relation between the effective area and the X-ray energy for various incident angles in GSC. The peak effective area is determined by the collimator slit area, whereas the lower and the higher limits of the energy band are determined by the detector efficiency. The incident-angle dependence of the lower energy cutoff is due to the path length of the beryllium film at the front of the detector gas cell.

The dispersion relation between the X-ray energy and the pulse height of the readout signal depends on the absorbed position in the detector, which is also dependent on the photon incident angle. The energy response builder calculates the effective area and the energy redistribution matrix for each X-ray incident angle.

4.3. Point Spread Function and Exposure Map

The angular resolution of the GSC and the SSC are determined by the detector position resolution and the collimator windows size defined by their slit width and pitch of the slat panels.

The point spread function (PSF) and the exposure map of reconstructed image from GSC and SSC data depend on the instrument response as well as the instantaneous attitude. The response builder for the image analysis calculate the PSFs and the exposure map from the attitude data and the instrument calibration data.

In the case of SSC, the pixel size of the CCD (0.025

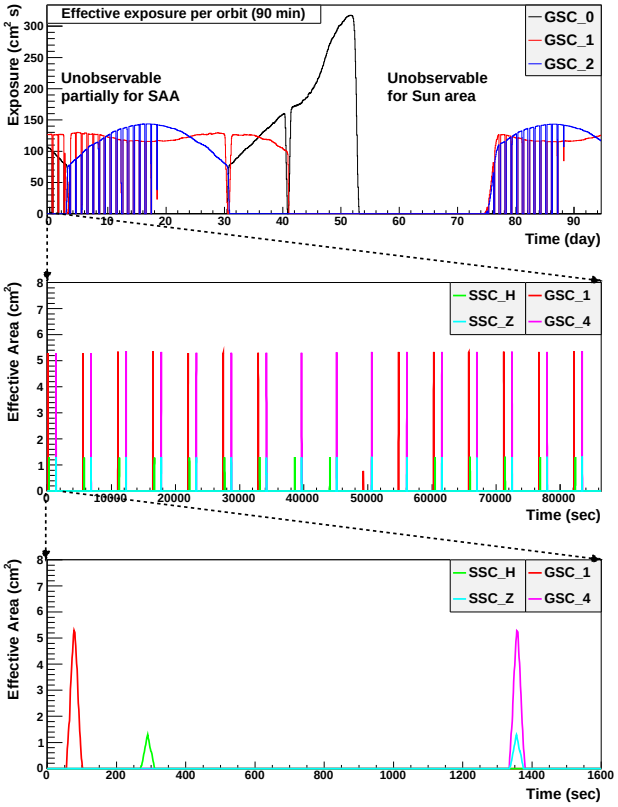

Fig. 4. Effective-are time variation for a given point source on the sky: Long-term variation of the average exposure time per orbit ($\approx$ 90 min) for each GSC counter unit (top). Effective-area variation within one day (middle). Effective-area variation in a scale of one scan (bottom).

mm) is much smaller than the slit width and the collimator pitch ($\simeq$ 2.3 mm). Thus, the profile of the collimator transmission function dominates the PSF.

In GSC, the position resolution of the gas counter depends on the X-ray energy, ranging from 1 to 4 mm within the energy band (Mihara et al. 2001). It is comparable to the slit width (3.7 mm) and the slat pitch (3.1 mm) of the GSC collimator. Thus, the detector resolution has to be taken into account. Figure 6 shows the expected PSFs for X-rays of 2 keV and 10 keV with incident angles of 2, 20, and 40 degree. The profile at 10 keV is obviously extended towards the incident angle. It is because the mean free path of these photons in the detector cannot be disregarded.

The exposure map is calculated from the effective-area map of the X-ray cameras, the ISS orbit and attitude data. Figure 7 shows the exposure maps of one GSC counter for one orbit and that of the entire 12 counters for one day. GSC covers 90% of the whole sky with an ISS-orbit cycle of $\sim$ 90 minutes.

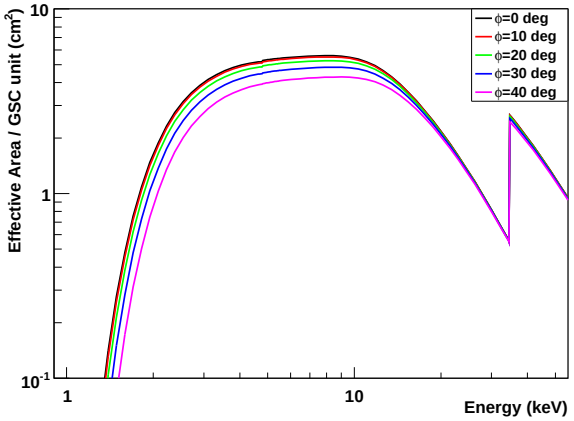

Fig. 5. Effective area of a GSC counter unit in the energy band of 1–50 keV for each X-ray incident angle of 0, 10, 20, 30, 40 degree.

5. Simulator

We are developing a MAXI observation simulator not only to study the scientific feasibility but also to examine the analysis software under development. The detail of the simulator is described in Eguchi et al. in this proceedings. Figure 8 and 9 show some results of all-sky image, light curves and energy spectra obtained from the simulated data of MAXI one-day observation.

6. Summary

We are building the standard analysis framework of MAXI data and developing the software which include programs for telemetry-data reduction, response builder, and observation simulator. The software will be used to process and analyze the archival products of MAXI data, which will be available after the MAXI mission is shifted to the normal operation phase. The status of the mission, information of the data archive and the latest software will be updated on the MAXI web site (http://maxi.riken.jp).

References

Eguchi, S., et al. in this proceedings (MAXI simulator)
Katayama, H., et al. 2005, Nucl. Instr. Meth. A541, 350-356
Kohama, M., et al. in this proceedings
Matsuoka, M., et al. 2007, Proc. SPIE 6686, 11-1-9
Mihara, T., et al. 2001, Proc. SPIE 4497, 173-186
Mihara, T., et al. in this proceedings (MAXI GSC)
Tomida, H., et al. in this proceedings (MAXI SSC)
Ueno, S., et al. 2004, Proc. SPIE 5488, 197-208
Ueno, S., et al. in this proceedings (MAXI mission overview)

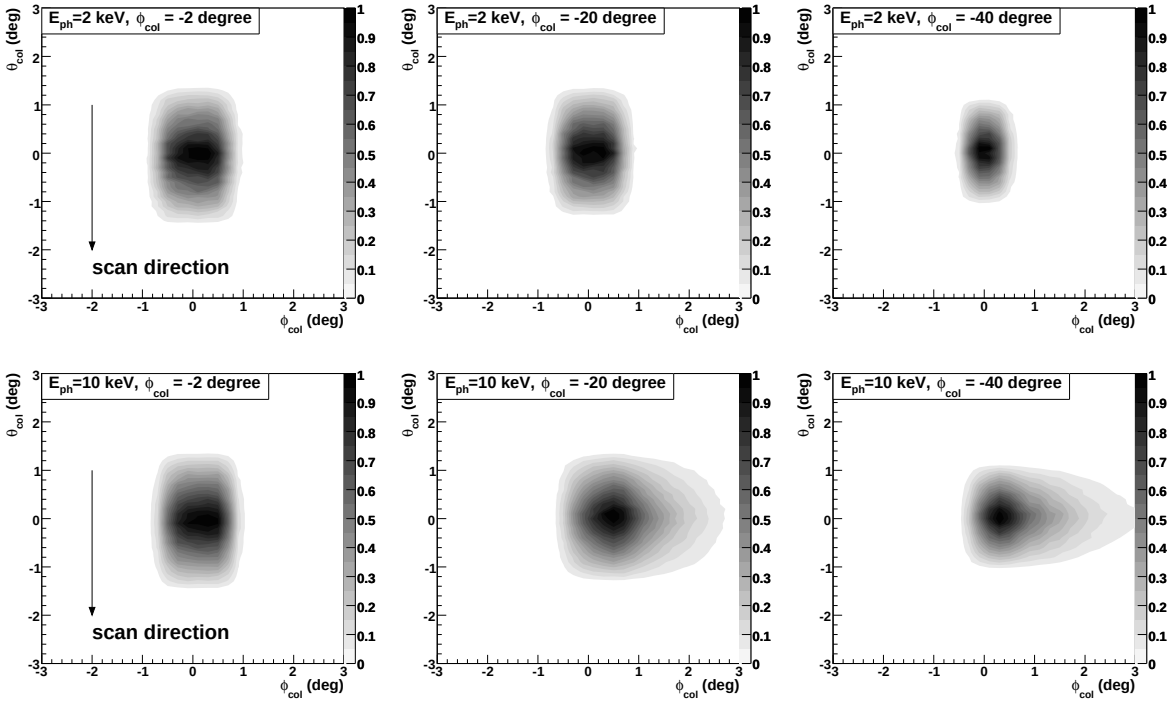

Fig. 6. Point Spread functions of a GSC camera for X-ray photons of 2-keV (top) and 10-keV (bottom) with an incident angle of 2° (left), 20° (center), and 40° (right).

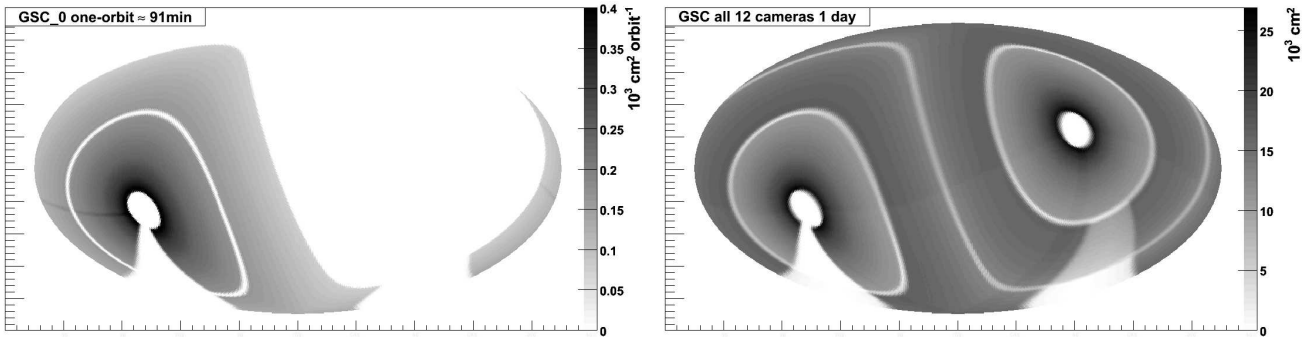

Fig. 7. All sky exposure map by one GSC-counter unit for one-orbit (left) and by entire 12 GSC-counter units for one-day (right). The uncovered area at the bottoms of the both figures corresponds to the Sun direction.

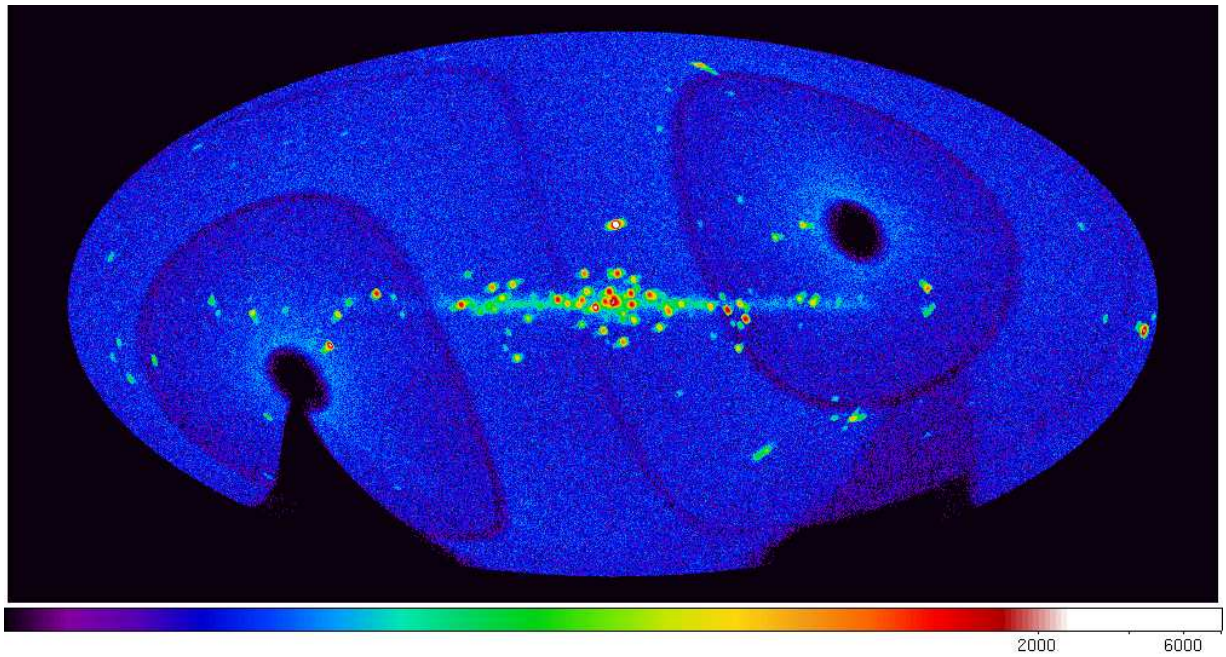

Fig. 8. Simulation of GSC observation of all-sky X-ray image for one day. Backgrounds by cosmic-ray particles are not included. The image of Figure 7 corresponds the exposure map for this data.

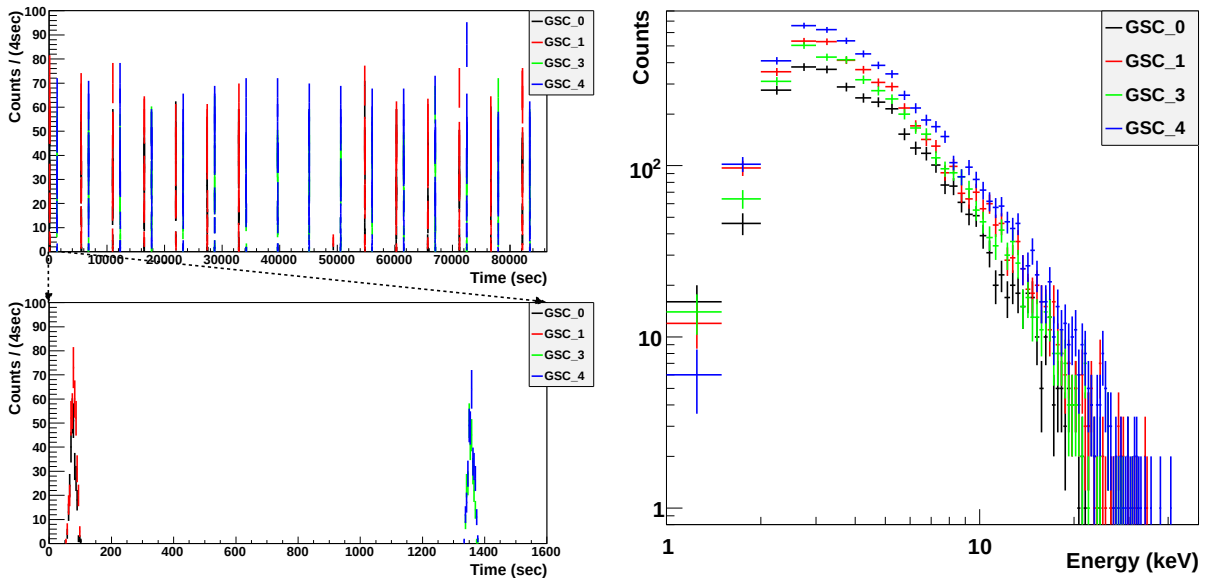

Fig. 9. Simulation of GSC observation of Crab nebula for one day. X-ray count rates by each GSC counter (left). Figure 4 corresponds to these response function. X-ray energy spectra by each GSC counter (right).